

Comparative Assessment of LiDAR Point Clouds Captured Using Inertial Labs RESEPI Gen-I-M2X and DJI Zenmuse L2 Sensors on UAS Platforms for Varying Terrain Conditions

Rami Tamimi¹, Baris Süleymanoğlu², Abdelgwad Elashry³, Charles Toth¹

¹ SPIN Laboratory, Department of Civil, Environmental and Geodetic Engineering,
The Ohio State University, Columbus, OH, USA 43210 – (tamimi.12, toth.2) @osu.edu

² Faculty of Civil Engineering, Department of Geomatics Engineering,
Yildiz Technical University, 34220 Istanbul, Turkey – bariss@yildiz.edu.tr

³ Computer Engineering Department, Faculty of Engineering Technology,
Elsewedy University of Technology, Egypt – abdelgwad.elashry@sut.edu.eg

KEY WORDS: UAS, LiDAR, PPK corrections, point cloud, surveying.

ABSTRACT:

Unmanned Aerial Systems (UAS) equipped with LiDAR sensors are increasingly used for topographic surveying and mapping due to their ability to generate high-quality point clouds and penetrate vegetation. While photogrammetry remains a common approach in UAS mapping, its limitations in vegetated environments—where it often struggles to accurately capture ground surface details—have led to the adoption of LiDAR. LiDAR, with its capability to penetrate vegetation, provides more precise terrain observations and detailed representations of the underlying ground surface, even in densely vegetated areas. This study compares the performance of two LiDAR systems: the RESEPI Gen-I-M2X sensor from Inertial Labs, mounted on a WingtraOne Gen II fixed-wing UAS using post-processed kinematic (PPK) corrections; and the Zenmuse L2 sensor integrated with the DJI Matrice 350 RTK, utilizing real-time kinematic (RTK) corrections with additional PPK adjustments based on observation files from a local Continuously Operating Reference Station (CORS) acting as the base. Both platforms were flown over the same area, with point clouds analyzed across three distinct conditions: open terrain, urban development, and wooded areas. A total of 135 GNSS-measured reference points were deployed, with 10 designated as ground control points (GCPs) to enhance vertical accuracy, while the remaining 125 points served as checkpoints for validation. Some checkpoints were located at the center of manhole covers, others at painted arrow markers on roadways, but the majority—especially those in wooded areas—were natural points without signalization. The Zenmuse L2 datasets were processed in DJI Terra, generating point clouds with and without GCP integration. In contrast, the RESEPI Gen-I-M2X datasets relied solely on PPK corrections, as the processing software does not support GCP integration. This study evaluates the accuracy and noise levels of the point clouds in varying environments, focusing on terrain representation by the LiDAR sensors. The findings provide insights into the strengths and limitations of each platform and correction strategy, offering guidance for selecting appropriate UAS LiDAR systems for specific surveying and mapping applications. This research contributes to the growing body of work on UAS LiDAR by highlighting key factors that influence data quality, including sensor selection, correction methods, and environmental conditions.

1. INTRODUCTION

LiDAR-equipped UAS platforms are transforming surveying by providing precise topographic data, especially in areas where traditional optical imagery encounters limitations, such as dense vegetation. Despite these advancements, achieving high accuracy remains challenging due to sensor limitations that affect positional data. Correction methods, including RTK, PPK, and GCP integration, are essential for enhancing both vertical and horizontal accuracy. Recent research provides valuable insights into sensor capabilities, correction strategies, and data quality across varying conditions.

Józków et al., (2016) identified that dual-frequency GNSS provides reliable positional data, though noise from Inertial Measurement Units (IMUs) can introduce vertical errors of up to 0.49 meters in LiDAR point clouds. They proposed solutions such as imagery-based trajectory reconstruction, vibration isolation, and simultaneous image-LiDAR acquisition to improve georeferencing accuracy. Lightweight MEMS-based IMUs remain prone to noise and bias (El-Sheimy, 2009), though advancements in MEMS technology are approaching tactical-grade performance (Hirose et al., 2015). Larger UAS platforms can carry high-grade IMUs but at the cost of added weight and expense (Yang and Chen, 2015). The development of lightweight LiDAR sensors, such

as the Hokuyo UTM-30LX (Kuhnert and Kuhnert, 2013), has further enhanced UAS mapping. High-performance sensors, including the Riegl UAVX-1 and Velodyne models like the HDL-32E and VLP-16, offer a balance between weight, data acquisition rate, and accuracy, making them ideal for UAS applications (Tulldahl and Larsson, 2014; Mandlbürger et al., 2015).

Hu et al., (2021) developed a low-cost UAS LiDAR system using the DJI Livox MID40 sensor, comparable to the Zenmuse L2. This sensor's performance was tested against higher-end models like the HESAI Pandar40, which we employ in this study. (Jaakkola et al., 2017) demonstrated the effectiveness of lightweight LiDAR systems, including the Sick LMS151 and Ibeo Lux, in forest applications. In coniferous forests, the Livox MID40 achieved vertical accuracy of 0.59 meters, though performance declined in broadleaf forests, with RMSE increasing to 1.63 meters. Similar challenges, including low intensity returns and narrow fields of view, were observed with earlier Velodyne Puck systems (Guo et al., 2017). Despite these limitations, the Livox MID40 captured both canopy and terrain surfaces effectively, making it suitable for forest management. In comparison, the HESAI Pandar40 provided superior data quality across diverse canopy conditions (Mandlbürger et al., 2015).

Kovanič et al., (2023) reviewed UAS platforms equipped with photogrammetry and LiDAR sensors, highlighting their ability to generate high-resolution spatial data. UAS with RTK/PPK systems achieved precise horizontal positioning, though vertical discrepancies were observed, consistent with findings from (Zeybek 2021) and (Tomaščík et al., 2019). Incorporating GCPs significantly improved vertical accuracy, reducing RMSE from 0.20–0.40 meters to below 0.15 meters (Štroner et al., 2021). Without GCPs, vertical RMSE fluctuated between 0.10 and 0.20 meters. Additionally, UAS equipped with Velodyne Puck VLP-16 sensors achieved point densities up to 50 points per square meter, with vertical RMSE values ranging between 0.10 and 0.15 meters (Brede et al., 2017).

PPK trajectory processing plays a key role in improving the accuracy of UAS LiDAR point clouds. (Oniga et al., 2023) demonstrated PPK georeferencing with the DJI Matrice 300 RTK and GeoSun GS-130X sensor, achieving corrections without requiring GCPs (Dreier et al., 2021). Flights conducted at 60 and 100 meters altitude (AGL) used 985 checkpoints to validate accuracy, yielding vertical RMSEs of 2 centimeters and 4 centimeters, respectively. Planimetric errors were 4.8 centimeters for the 60-meter flight and 6.5 centimeters for the 100-meter flight. Total errors were 5.3 centimeters and 7.5 centimeters for the lower and higher altitudes, respectively, underscoring the effectiveness of PPK in reducing positional discrepancies (Elamin et al., 2022).

Recent advancements in UAS LiDAR technology, particularly the DJI Zenmuse L2 sensor, are reshaping surveying by enhancing data collection accuracy and efficiency. (Tamimi and Toth, 2024) evaluated the Zenmuse L2's performance using the Matrice 350 with RTK corrections, reporting an RMSE of 0.07 meters in open areas, suitable for infrastructure projects. However, in densely vegetated areas, RMSE increased to 0.21 meters, reflecting the challenges of penetrating foliage and managing multiple returns. These findings align with previous studies, where (Sun et al., 2024) highlighted the Zenmuse L2's precision in landslide monitoring, achieving an RMSE of 0.06 meters. Similarly, (Salach et al., 2018) demonstrated the advantages of UAS LiDAR for Digital Terrain Model (DTM) creation, with LiDAR maintaining superior accuracy under canopy cover and achieving an RMSE of 0.05 meters.

This study builds on prior research by directly comparing the performance of two UAS LiDAR systems—the RESEPI Gen-I-M2X sensor with PPK corrections and the Zenmuse L2 sensor with RTK corrections—across various environmental conditions. Both systems were flown over the same area, adhering to consistent data collection and processing protocols to ensure comparability. Using 135 GNSS-measured points, including 10 GCPs and 125 checkpoints, we evaluated the impact of correction strategies on vertical accuracy. The following methodology section outlines the flight procedures, data acquisition techniques, correction processes, and software workflows used to analyze the point clouds, providing a clear framework for interpreting the study's results.

2. MATERIALS & METHODOLOGY

2.1 Study Area

The study area for this research spans approximately 225 acres (91 hectares) and covers a significant portion of the small town of Utica, located in metro Detroit, Michigan. This area offers a diverse environment, ranging from open fields to a compact

urban downtown, as well as natural landscapes, including a creek surrounded by dense tree coverage. The selection of this area provides an ideal setting to evaluate the performance of LiDAR sensors across varying conditions within a single dataset.

The mixed environment enables testing of sensor capabilities under multiple scenarios, such as capturing open spaces, navigating urban obstructions, and penetrating dense vegetation. The urban areas allow assessment of the sensors' ability to map hard surfaces like roads and building facades, while the creek and forested sections test their capacity to penetrate canopy cover and accurately capture ground data. Conducting the study in this heterogeneous environment ensures a thorough evaluation of the sensors and helps identify processing strategies to optimize data accuracy under varying conditions.



Figure 1. Study Area, Utica, MI, USA

2.2 Hardware



2.2.1 WingtraOne Gen II: The RESEPI Gen-I-M2X LiDAR sensor was mounted on a fixed-wing vertical take-off and landing (VTOL) drone. This drone was chosen for its efficiency in covering large areas and its compatibility with the sensor's payload requirements. To achieve precise georeferencing, we used PPK corrections, with an Emlid Reach RS2+ serving as the base station to log raw observation data. Post-processing was conducted using PCMasterPro software from Inertial Labs to correct the flight trajectories. The WingtraOne Gen II, with a flight time of up to 59 minutes, supports extended missions over the 91-hectare study area. Its VTOL capability allows it to take off and land in confined spaces, making it well-suited for operations across diverse environments, including urban areas and open fields.

2.2.2 DJI Matrice 350 RTK: A quadcopter was used to carry the Zenmuse L2 LiDAR sensor. This drone supports RTK technology, enabling precise real-time georeferencing by minimizing positional errors. It connects to the Michigan Department of Transportation (MDOT) CORS network to obtain real-time corrections. With a flight time of up to 55 minutes and sufficient payload capacity, the Matrice 350 RTK can complete extended missions while carrying the LiDAR sensor. Its integration with DJI Terra software further simplifies mission planning, data acquisition, and processing.

2.2.3 RESEPI Gen-I-M2X: Developed by Inertial Labs, the RESEPI is a compact LiDAR system integrated with a GNSS-aided inertial navigation system (INS). It uses the HESAI puck sensor, which features 16 channels, a 360-degree horizontal field of view, and a 40.3-degree vertical field of view. The system can capture up to 640,000 points per second, offers three return options per laser pulse, and has a maximum range of 300 meters. Its range accuracy is 1 cm at 150 meters, with a horizontal beam divergence of 0.21° and a vertical beam divergence of 0.047°. Weighing 490 grams, the RESEPI was mounted on the WingtraOne Gen II for aerial LiDAR surveys over the study area. It employs its PPK corrections, with a separate GNSS antenna attached to the sensor for trajectory data collection. This data was later corrected using an Emlid Reach RS2+ base station.

2.2.4 Zenmuse L2: Developed by DJI, the Zenmuse L2 integrates a GNSS-aided INS, offering a 70-degree horizontal field of view and a 3-degree vertical field of view. The system captures up to 240,000 points per second, provides five return options per laser pulse, and has a maximum range of 450 meters. Its range accuracy is 2 cm at 150 meters, with a horizontal beam divergence of 0.0115° and a vertical beam divergence of 0.0344°. Weighing approximately 905 grams, the Zenmuse L2 was mounted on the DJI Matrice 350 RTK for data acquisition, utilizing the Matrice's GNSS antenna to receive RTK corrections, as the Zenmuse L2 lacks a dedicated GNSS antenna. After the flight, the entire system's trajectories were refined using PPK corrections from logging data provided by a local CORS base station to ensure the highest level of accuracy for trajectory calculations. These specifications are summarized in Table 1.

Table 1. Specification comparison between Inertial Labs RESEPI M2X and DJI Zenmuse L2.

| Device Name | RESEPI M2X | ZENMUSE L2 |
|----------------------------------|---|---|
| Appearance |  |  |
| Maximum Range | 300 m | 450 m |
| Range Accuracy | 1 cm @ 150 m | 2 cm @ 150 m |
| Number of Returns | 3 | 5 |
| Data Points Generated Per Return | 640,000 pts/s | 240,000 pts/s |
| Field of View | 360° (H) 40.3° (V) | 70° (H) 3° (V) |
| Beam Divergence | 0.21° (H) 0.047° (V) | 0.0115° (H) 0.0344° (V) |
| Weight | 490 g | 905 ± 5 g |

2.3 Software

2.3.1 PCMasterPro: This software, developed by Inertial Labs, processes data collected from the RESEPI Gen-I-M2X sensor. It manages PPK corrections by integrating GNSS data from a base station with the sensor's inertial data, ensuring accurate georeferencing. However, PCMasterPro lacks the capability to incorporate GCPs into its workflow, which limits flexibility for validating or enhancing positional accuracy beyond what PPK corrections provide. Consequently, the generated point cloud relies solely on PPK corrections without the inclusion of GCPs.

2.3.2 DJI Terra: This software processes data collected from the Zenmuse L2 sensor. One limitation of DJI Terra is that, while it supports the integration of GCPs, it applies corrections only in the vertical direction. Accurately measuring the horizontal position of a LiDAR echo presents inherent challenges due to factors such as beam divergence, the angle of incidence, and the positional uncertainty of each pulse, which complicate precise horizontal adjustments. This limitation can affect horizontal accuracy improvements, making it less suitable for projects that demand high-precision horizontal adjustments. Nevertheless, DJI Terra's compatibility with DJI hardware and its ability to generate accurate vertical corrections make it a valuable tool for processing LiDAR data in various environments. Two point clouds were generated from the L2 on DJI Terra: the first uses only PPK corrections with no GCPs, while the second integrates both 10 GCPs and PPK corrections.

2.3.3 CloudCompare: A free open-source software, to analyze profiles of the different point clouds, identify vertical discrepancies, and measure sensor noise. This software facilitates efficient comparison and assessment of point cloud data from various sources.

2.4 Methodology

The methodology for this study focuses on generating three point clouds, georeferencing them, and analyzing their accuracy and noise levels. Data was collected using two LiDAR systems: (1) RESEPI Gen-I-M2X with PPK corrections and no GCPs, (2) Zenmuse L2 with PPK corrections and no GCPs, and (3) Zenmuse L2 with PPK corrections along with vertical GCPs. Each dataset was produced by flying the sensors over the same 225-acre (91-hectare) study area, ensuring consistent environmental conditions across all data collections.

We began by setting up an Emlid Reach RS2+ over a network RTK GNSS-measured point, which served as the base station for PPK corrections. The base station recorded raw GNSS observation data throughout the mission. After mounting the sensor, we calibrated the system to ensure precise data collection, including sensor alignment checks and verifying the connection between the RESEPI Gen-I-M2X LiDAR system and the GNSS-aided INS. The WingtraOne Gen II was flown at an altitude of 300 feet AGL, maintaining approximately 40% overlap between flight paths to ensure comprehensive coverage of the 91-hectare study area. The average flight speed was set at 17 miles per hour (27.4 km/h), balancing survey efficiency with data density for high-resolution mapping.

Once data collection was complete, the base station was powered down, and data from both the drone and base station

were uploaded to PCMasterPro for processing. PPK corrections were applied to the flight trajectories using the base station GNSS data, ensuring accurate positioning. A final point cloud was generated, relying solely on PPK corrections for georeferencing, with no GCPs applied.

The Matrice 350 RTK was connected to the MDOT CORS network to receive RTK corrections during the flight, which provided enhanced trajectory accuracy for later georeferencing of the Zenmuse L2 LiDAR data by reducing positional errors. The flight was conducted at a lower altitude of 260 feet AGL, with a 40% overlap between flight paths to improve data density and accuracy. The average speed was 11 miles per hour (18 km/h). This configuration, feasible with the Matrice 350 RTK quadcopter but not with fixed-wing platforms like the WingtraOne Gen II, offered an inherent advantage in data resolution due to the ability to maintain a more controlled and precise flight path.

An Emlid Reach RS3 GNSS receiver was used to collect 10 GCPs and 125 checkpoints across the study area, ensuring accurate georeferencing and validation of the LiDAR data. The GCPs were intended to enhance the vertical accuracy of the point cloud generated by the Zenmuse L2 sensor, while the checkpoints were used to validate the final output. Before processing in DJI Terra, the base station's observation file was updated with RTK corrections to ensure that PPK corrections were applied to all trajectory calculations, optimizing accuracy across the system.

The collected LiDAR data was processed twice using DJI Terra software to evaluate the effect of GCPs on accuracy. In the first processing, only PPK corrections were applied without GCP integration, creating the initial point cloud. For the second processing, both PPK corrections and the 10 GCPs were applied to improve vertical accuracy, resulting in the final point cloud. Comparing these two datasets (PPK without GCPs and PPK with GCPs) enabled a comprehensive analysis of the LiDAR system's accuracy and performance under different correction conditions.

2.4.1 Point Cloud Generation and Trajectory Correction: For the RESEPI Gen-I-M2X system, PPK corrections were applied to enhance georeferencing accuracy by synchronizing the GNSS data collected on the drone with reference data from the Emlid Reach RS2+ base station. The raw GNSS observations were combined with inertial data using PCMasterPro software to generate precise flight trajectories.

For the Zenmuse L2 sensor, PPK corrections from the M350 were applied during the flight. These corrections were used to generate two datasets: one using only PPK corrections and another incorporating 10 vertical GCPs to further improve accuracy.

2.4.2 Georeferencing of LiDAR Point Clouds: The LiDAR point clouds were transformed from their local coordinate frames to a global reference frame for accurate mapping. The transformation follows:

$$P_g = R_{bg}R_{sb}P_s + T_{bg}$$

where P_g is the georeferenced point in the global frame projected into UTM Zone 17N, R_{bg} is the rotation matrix from the body frame to the global frame, R_{sb} is the rotation matrix from the sensor frame to the body frame, P_s is the point in the

sensor frame, T_{bg} is the translation from the sensor origin to the global frame.

2.4.3 Accuracy Assessment: The accuracy of the point clouds was evaluated using 135 GNSS-measured points, consisting of 10 GCPs and 125 checkpoints. For each point cloud, the RMSE was calculated to quantify the accuracy of the vertical components:

$$RMSE = \sqrt{\frac{1}{n} \sum_{i=1}^n (P_{LiDAR,i} - P_{GNSS,i})^2}$$

where $P_{LiDAR,i}$ is the point in the LiDAR point cloud, $P_{GNSS,i}$ is the corresponding GNSS-measured check point, and n is the total number of points. A corresponding point refers to the GNSS-measured checkpoint nearest to each LiDAR point, matched by spatial proximity to minimize vertical positional differences.

This accuracy assessment was performed on three datasets:

1. **RESEPI with PPK and no GCPs (RESEPI):** Evaluates the performance of PPK corrections alone.
2. **Zenmuse L2 with PPK and no GCPs (L2_noGCP):** Measures RTK correction performance without GCPs. PPK added after flight.
3. **Zenmuse L2 with PPK and vertical GCPs (L2_withGCP):** Assesses how vertical GCPs improve elevation accuracy.

2.4.4 Noise Analysis: In addition to assessing accuracy, noise levels were analyzed by extracting profiles and cross-sections from the point clouds, with a focus on flat or planar areas to better understand noise on uniform surfaces. CloudCompare, a free open-source software, was used to compute the standard deviation of point distributions within these regions, providing insights into the consistency and reliability of data captured in low-relief areas.

$$\sigma_{noise} = \sqrt{\frac{1}{n-1} \sum_{i=1}^n (P_i - \bar{P})^2}$$

where P_i is an individual point in the profile, \bar{P} is the mean position of the points, and n is the number of points. This analysis helped identify inconsistencies in point density and distribution.

3. RESULTS

3.1 Point Clouds

As a result of these procedures, dense point clouds were generated for all three datasets. Specifically, the L2_noGCP and L2_withGCP datasets yielded approximately 315 million points, with an average point density of 418 points per square meter. In contrast, the point cloud data obtained using the RESEPI M2X consisted of approximately 80 million points, with an average point density of 70 points per square meter. These results show that, while the Zenmuse L2 datasets had nearly identical point counts and densities, they were significantly higher than those produced by the RESEPI M2X.

Figure 2 illustrates the point cloud data visualized from all three systems. As shown, despite following the same flight

trajectory, the RESEPI M2X captured data over a larger area than the Zenmuse L2. This broader coverage, enabled by RESEPI's 360-degree horizontal field of view, can improve operational efficiency in applications requiring extensive area mapping with fewer flight lines. Furthermore, the RESEPI M2X's data density across this extended area provides greater detail of terrain features, offering potential advantages for large-scale surveying tasks where spatial extent and data continuity are crucial.

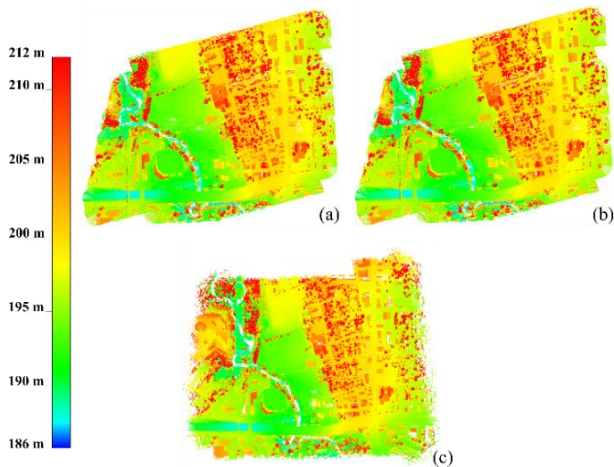


Figure 2. The datasets obtained from all three data sources are visualized as follows:
a) L2_noGCP, b) L2_withGCP, c) RESEPI

3.2 Noise Removal and Accuracy Assessment

A three-stage framework was implemented to conduct the accuracy assessment. In the first stage, the Statistical Outlier Removal (SOR) filter was applied to detect and remove outliers in the dataset, minimizing extreme deviations and enhancing the precision of subsequent filtering operations (Rusu and Cousins, 2011). Next, the data was filtered using the well-known Cloth Simulation Filtering (CSF) algorithm, recognized for its effectiveness in distinguishing ground from non-ground points (Zhang et al., 2016). The study area was divided into three segments: open, urban, and forested areas.

After extensive testing, the CSF parameters were optimized as follows: Cloth Resolution, number of iterations, and threshold values were set to 1.5, 500, and 0.4 for the open area; 0.4, 500, and 0.7 for the forested area; and 1, 500, and 0.5 for the urban area.

The accuracy assessment of the LiDAR datasets was conducted across three environmental settings: open, urban, and forested areas, as illustrated in Figures 3, 4, and 5. In the open environment (Figure 3), which includes a football field and track with 91 checkpoints, the L2 datasets demonstrated robust performance, achieving RMSE values of 0.06 meters (L2_noGCP) and 0.04 meters (L2_withGCP). In contrast, the RESEPI M2X dataset displayed a higher RMSE of 0.10 meters, indicating challenges in accurately capturing grassy surfaces.



Figure 3. Reference checkpoints in an open environment.

In the urban environment (Figure 4), where 12 checkpoints were distributed, the RESEPI M2X achieved the lowest RMSE at 0.02 meters, underscoring its reliability in structured, low-relief settings. The L2 datasets also performed well, with RMSE values of 0.09 meters (L2_noGCP) and 0.05 meters (L2_withGCP). Points 3 and 7 served as GCPs in the L2_withGCP dataset, likely contributing to the enhanced vertical accuracy observed in urban areas.

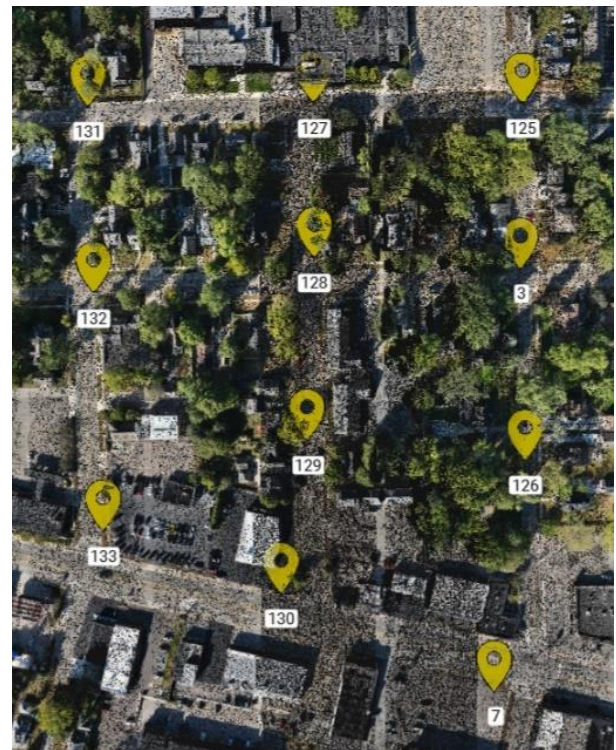


Figure 4. Reference checkpoints in an urban environment.

The forested environment (Figure 5), with 9 checkpoints, presented substantial challenges for both systems due to dense canopy cover, which limited GNSS signal reception. In this setting, the L2_noGCP and L2_withGCP datasets yielded RMSE values of 0.22 meters and 0.19 meters, respectively, while the RESEPI M2X recorded a higher RMSE of 0.27 meters. These findings underscore the reduced efficacy of both

systems in heavily vegetated areas, where point cloud accuracy is inherently compromised by limited GNSS signal penetration. These results, summarized in Table 2 and visualized in Figure 6, emphasize the importance of sensor-specific considerations based on environmental complexity and required accuracy.



Figure 5. Reference checkpoints in a forest environment.

Table 2. Vertical accuracy values calculated for each of the three datasets in all three scenarios.

| Dataset | Open | Urban | Forest |
|------------|--------|--------|--------|
| L2_noGCP | 0.06 m | 0.09 m | 0.22 m |
| L2_withGCP | 0.04 m | 0.05 m | 0.19 m |
| RESEPI M2X | 0.10 m | 0.02 m | 0.27 m |

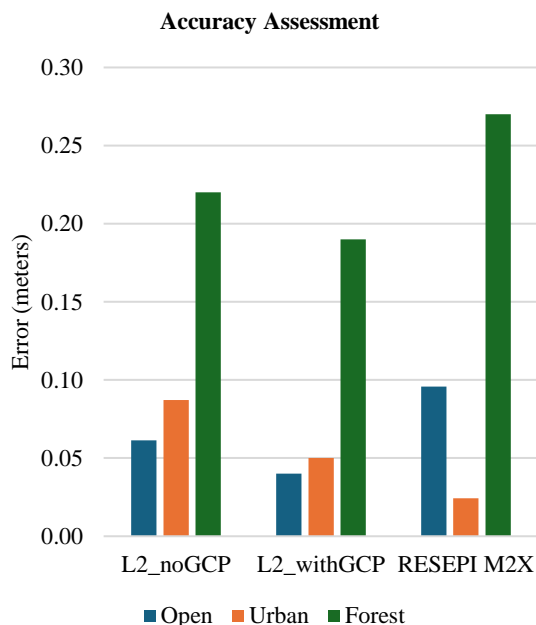


Figure 6. Visual representation of the error levels between the datasets in various environments.

3.3 Visual Accuracy Analyses with Profiles

In addition to quantitative analyses, a visual comparison was performed to assess data quality differences between the two consumer-grade LiDAR systems. Figure 7 presents cross-sections extracted from a forested area for each dataset, highlighting the capture of both the tree canopy and underlying ground surface. The L2_noGCP and L2_withGCP datasets exhibit a high level of consistency, indicating stable performance in capturing both vegetation and ground features. In contrast, the RESEPI M2X dataset displays variability in its

ability to detect finer details, such as leaves and small branches; in some cases, it captured these features with greater clarity than the Zenmuse L2, while in others, they were absent. This variability in RESEPI's data may reflect differences in sensor sensitivity and point density, influencing its effectiveness in densely vegetated areas.

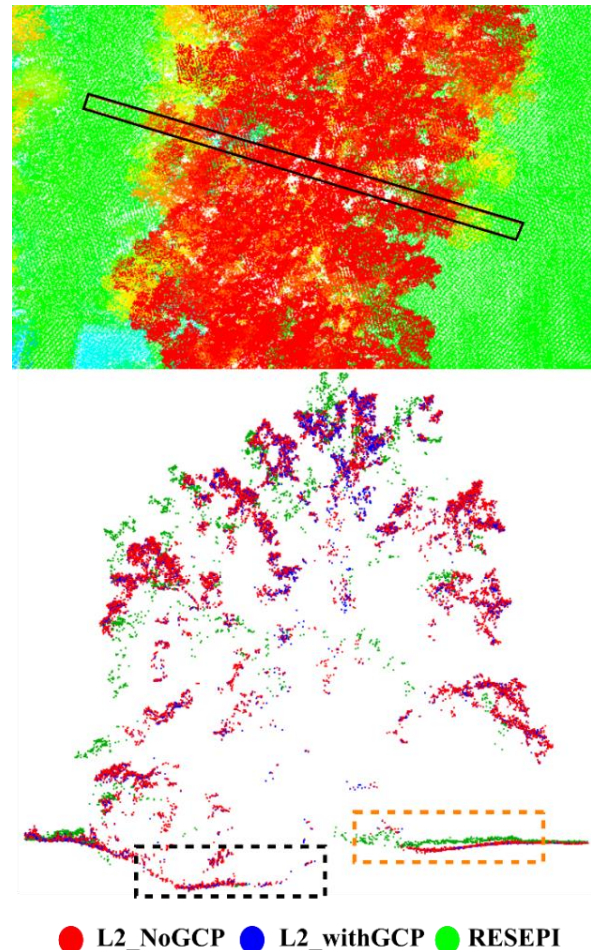


Figure 7. Cross-sections obtained from the forested area

In the area highlighted by the red dashed lines on the bottom-right, the RESEPI M2X captured a higher density of points, demonstrating its capability to detect more surface detail in certain regions. Conversely, in the area marked by the black dashed lines on the bottom-left, RESEPI recorded fewer points compared to the Zenmuse L2. This variability suggests that RESEPI's performance may fluctuate based on terrain characteristics or vegetation density, affecting its consistency in delivering uniform data coverage. These differences in point density underscore the importance of considering specific environmental conditions when selecting LiDAR systems for detailed terrain mapping.

Figure 8 presents cross-sections extracted from the roof of a house, showing that all three systems were able to accurately define the roof structure. Additionally, Figure 9 visualizes a segment of data on an electricity pole and a power line cable. The Zenmuse L2 successfully detected both elements, while the RESEPI M2X did not, likely due to its lower point density resulting from differences in sensor specifications and operational parameters. This highlights the importance of considering sensor characteristics and flight settings when aiming to capture fine details.

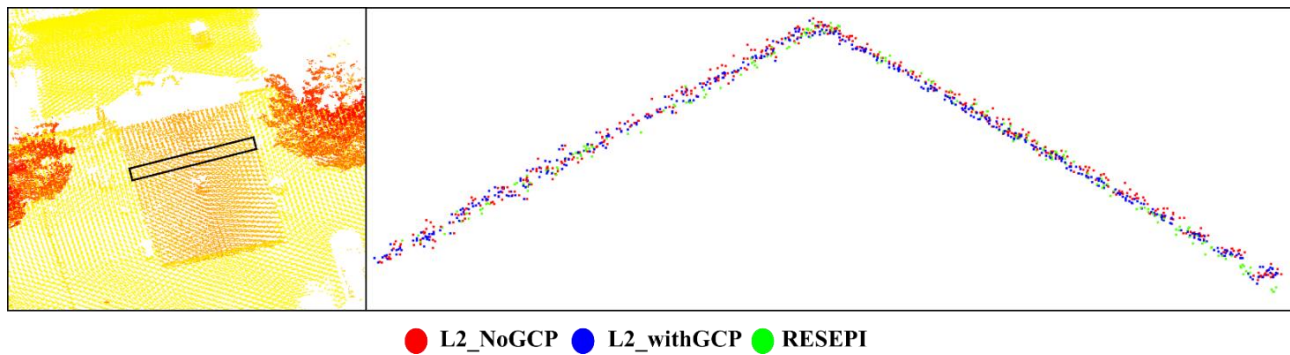


Figure 8. Cross-section obtained from the roof of the house

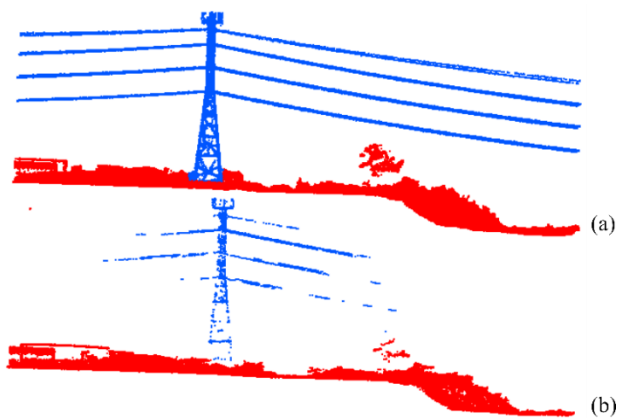


Figure 9. Electricity pole and power lines obtained with a) the Zenmuse L2, and b) the RESEPI M2X

4. DISCUSSION AND CONCLUSION

This study highlights performance differences between two consumer-grade LiDAR systems, the RESEPI Gen-I-M2X and Zenmuse L2, flown over the same study area on different UAS platforms. The Zenmuse L2 datasets, achieving a point density of 418 points per square meter, demonstrated significantly higher densities than the RESEPI M2X's 70 points per square meter, primarily due to differences in the number of returns, flight altitude, and speed. Consequently, the Zenmuse L2 more effectively captured fine linear features, such as power lines, suggesting it may be better suited for projects requiring high-detail mapping. Conversely, the RESEPI M2X may be advantageous for broader, lower-resolution surveys where extensive coverage is prioritized.

Despite its lower point density, the RESEPI M2X performed well in specific scenarios. For instance, in wooded areas, it detected canopy features that the Zenmuse L2 missed, indicating potential strengths in capturing certain vegetation elements. However, its performance was inconsistent, and it did not reliably detect these features across the entire dataset. In contrast, the Zenmuse L2, with its higher point density, excelled at capturing linear objects, such as power lines and electricity poles, while the RESEPI M2X either missed or captured these features with reduced clarity. This difference underscores the impact of point density on detecting fine, linear objects and highlights the Zenmuse L2's suitability for tasks requiring precise detection of narrow or thin structures.

The RMSE analysis further illustrates accuracy differences between the two systems across various environments. Overall, the Zenmuse L2 achieved lower RMSE values,

particularly in open and forested areas, with minor improvements from GCP integration (0.06 m without GCPs vs. 0.04 m with GCPs in open areas). In urban settings, however, the RESEPI M2X outperformed the Zenmuse L2, achieving an RMSE of 0.02 m. The inability to integrate GCPs with the RESEPI dataset, due to PCMasterPro limitations, may have affected its accuracy in other environments, emphasizing the importance of GCP compatibility for high-precision mapping.

From a practical perspective, the RESEPI M2X's ability to cover larger areas due to its higher altitude and fixed-wing platform may be advantageous for large-scale surveys. However, its reduced point density and variability in accuracy could limit its effectiveness in projects requiring high precision or detailed feature detection. In contrast, the Zenmuse L2's lower flight altitude, slower speed, and higher point density make it more suitable for tasks involving detailed feature extraction, particularly in urban areas or environments with complex infrastructure.

This study compared the performance of two LiDAR systems, the RESEPI Gen-I-M2X and Zenmuse L2, mounted on UAS platforms, focusing on point cloud generation, accuracy, and object detection capabilities. The results demonstrate that the Zenmuse L2, with its higher point density and slightly better RMSE values, is better suited for projects requiring high-precision data collection, particularly for detecting small or narrow objects like power lines. However, the RESEPI M2X exhibited certain advantages, notably in capturing some vegetation features, although it fell short in overall accuracy and point density.

The inclusion of GCPs in the Zenmuse L2 dataset contributed to a modest improvement in vertical accuracy, whereas the lack of GCP integration in the RESEPI dataset, due to software limitations, restricted its accuracy. Future research could explore the impact of GCP integration for the RESEPI M2X, potentially using the M2X on a quadcopter like the M350, or employ advanced post-processing techniques to enhance both horizontal and vertical accuracy.

ACKNOWLEDGEMENT

We extend our gratitude to Wingtra, DJI Enterprise, Inertial Labs, and Emlid for providing the hardware and software essential to our research. Their support and contributions were instrumental to the success of this project.

REFERENCES

- Józków, Grzegorz, Charles Toth, and Dorota Grejner-Brzezinska. "UAS topographic mapping with velodyne LiDAR sensor." *Isprs annals of the photogrammetry, remote sensing and spatial information sciences* 3 (2016): 201-208.
- El-Sheimy, N., 2009. Emerging MEMS IMU and its impact on mapping applications. *Photogrammetric Week*, Stuttgart, Germany.
- Yang, B., Chen, C., 2015. Automatic registration of UAV-borne sequent images and LiDAR data. *ISPRS Journal of Photogrammetry and Remote Sensing*, 101, pp. 262-274.
- Hirose, M., Xiao, Y., Zuo, Z., Kamat, V. R., Zekkos, D., Lynch, J., 2015. Implementation of UAV localization methods for a mobile post-earthquake monitoring system. 2015 IEEE Workshop on Environmental, Energy and Structural Monitoring Systems (EESMS), July 9-10, 2015, pp. 66-71.
- Kuhnert, K.D., Kuhnert, L., 2013. Light-weight sensor package for precision 3D measurement with micro UAVs e. g. powerline monitoring. *International Archives of the Photogrammetry, Remote Sensing and Spatial Information Sciences*, XL-1/W2, pp. 235–40.
- Mandlbauer, G., Pfennigbauer, M., Riegl, U., Haring, A., Wieser, M., Glira, P., Winiwarter, L., 2015. Complementing airborne laser bathymetry with UAV-based lidar for capturing alluvial landscapes. *Proceedings of SPIE 9637, Remote Sensing for Agriculture, Ecosystems, and Hydrology XVII*, 96370A, October 14, 2015, Toulouse, France, pp. 1-14.
- Tulldahl, H. M., Larsson, H., 2014. Lidar on small UAV for 3D mapping. *Proceedings of SPIE Security+ Defence conference, International Society for Optics and Photonics*, pp. 925009- 925009.
- Hu, Tianyu, et al. "Development and performance evaluation of a very low-cost UAV-LiDAR system for forestry applications." *Remote Sensing* 13.1 (2020): 77.
- Jaakkola, A., Hyypä, J.; Yu, X.; Kukko, A.; Kaartinen, H.; Liang, X.; Hyypä, H.; Wang, Y. Autonomous Collection of Forest Field Reference—The Outlook and a First Step with UAV Laser Scanning. *Remote Sens.* 2017, 9, 785.
- Guo, Q.; Su, Y.; Hu, T.; Guan, H.; Jin, S.; Zhang, J.; Zhao, X.; Xu, K.; Wei, D.; Kelly, M.; et al. Lidar boosts three-dimensional ecological observations and modelling: A review and perspective. *IEEE Geosci. Remote Sens. Mag.* 2020.
- Kovanič, Ľudovít, et al. "Review of photogrammetric and lidar applications of UAV." *Applied Sciences* 13.11 (2023): 6732.
- Zeybek, M. Accuracy assessment of direct georeferencing UAV images with onboard global navigation satellite system and comparison of CORS/RTK surveying methods. *Meas. Sci. Technol.* 2021, 32, 065402.
- Tomašík, J.; Mokroš, M.; Surový, P.; Grznárová, A.; Merganič, J. UAV RTK/PPK Method—An Optimal Solution for Mapping Inaccessible Forested Areas? *Remote Sens.* 2019, 11, 721.
- Štroner, M.; Urban, R.; Seidl, J.; Reindl, T.; Brouček, J. Photogrammetry Using UAV-Mounted GNSS RTK: Georeferencing Strategies without GCPs. *Remote Sens.* 2021, 13, 1336.
- Brede, B.; Lau, A.; Bartholomeus, H.M.; Kooistra, L. Comparing RIEGL RiCOPTER UAV LiDAR Derived Canopy Height and DBH with Terrestrial LiDAR. *Sensors* 2017, 17, 2371.
- Oniga, Valeria-Ersilia, et al. "Enhancing LiDAR-UAS Derived Digital Terrain Models with Hierarchic Robust and Volume-Based Filtering Approaches for Precision Topographic Mapping." *Remote Sensing* 16.1 (2023): 78.
- Dreier, A.; Janßen, J.; Kuhlmann, H.; Klingbeil, L. Quality Analysis of Direct Georeferencing in Aspects of Absolute Accuracy and Precision for a UAV-Based Laser Scanning System. *Remote Sens.* 2021, 13, 3564.
- Elamin, A.; Abdelaziz, N.; El-Rabbany, A. A GNSS/INS/LiDAR Integration Scheme for UAV-Based Navigation in GNSS-Challenging Environments. *Sensors* 2022, 22, 9908.
- Tamimi, Rami, and Charles Toth. "Accuracy Assessment of UAV LiDAR Compared to Traditional Total Station for Geospatial Data Collection in Land Surveying Contexts." *The International Archives of the Photogrammetry, Remote Sensing and Spatial Information Sciences* 48 (2024): 421-426.
- Sun, Jianwei, et al. "Unmanned Aerial Vehicles (UAVs) in Landslide Investigation and Monitoring: A Review." *Drones* 8.1 (2024): 30.
- Salach, Adam, et al. "Accuracy assessment of point clouds from LiDAR and dense image matching acquired using the UAV platform for DTM creation." *ISPRS International Journal of Geo-Information* 7.9 (2018): 342.
- Rusu, R. B., & Cousins, S. (2011, May). 3d is here: Point cloud library (pcl). In 2011 IEEE international conference on robotics and automation (pp. 1-4). IEEE.
- Zhang, W., Qi, J., Wan, P., Wang, H., Xie, D., Wang, X., & Yan, G. (2016). An easy-to-use airborne LiDAR data filtering method based on cloth simulation. *Remote sensing*, 8(6), 501.
- Gao, X., & Su, W. (2023). Research on Modeling Method of Digital Elevation Model for Dense Matching Point Cloud Images in Complex Environments. *Academic Journal of Computing & Information Science*, 6(13), 76-81.
- Hengl, T. Finding the Right Pixel Size. *Computers & Geosciences*, Vol. 32, No. 9, 2006, pp. 1283–1298.